Histol Histopathol (2023) 38: 475-485

http://www.hh.um.es

Histology and Histopathology
From Cell Biology to Tissue Engineering

ORIGINAL ARTICLE **Open Access**

Up-regulation of oxidized low-density lipoprotein receptor 1 correlates with decreased miR-106b-5p, miR-93-5p, miR-3129-5p, miR-199b-3p, and miR-4465, higher recurrence rate, and poor prognosis in ovarian cancer

Jun Liu[1], Ya Zeng[2] and Lang Zheng[1]

[1]Department of Gynecology, Hainan General Hospital, Hainan Affiliated Hospital of Hainan Medical University, Haikou and [2]Department of Gynecology, Affiliated Hospital of Chengdu University, Chengdu, PR China

Summary. Background. MicroRNAs (miRNAs) are widely involved in cell metabolism, and their abnormal expression is involved in the regulation of ovarian cancer development, metastasis, and recurrence. The current study aimed to explore the potential mechanism and prognostic value of miRNAs related to the targeted regulation of oxidized low-density lipoprotein receptor 1 (OLR1) expression in ovarian cancer.

Methods. A prospective study was conducted including 132 ovarian cancer patients. Patients were followed up for 36 months. The dual-luciferase reporter gene detection was used to verify the targeting relationship between miRNA and OLR1. Cell Counting Kit-8 assay, flow cytometric analysis, transwell migration, and invasion assays were performed to address the malignant biological behaviors of ovarian cancer cells.

Results. OLR1 protein and gene expression levels were significantly higher in ovarian cancer tissues and cell lines than in adjacent tissues and normal ovarian epithelial cells. OLR1 depletion facilitated apoptosis and impeded cell proliferation, migration, and invasion in ovarian cancer. Predictive software and dual-luciferase reporter assays showed that miR-106b-5p, miR-93-5p, miR-3129-5p, miR-199b-3p, and miR-4465 targeted OLR1 expression. Functionally, the introduction of miR-106b-5p, miR-93-5p, miR-3129-5p, miR-199b-3p, and miR-4465 mimics abrogated the aggressive phenotype in ovarian cancer cells. Lastly, compared with adjacent tissues, the levels of miR-106b-5p, miR-93-5p, miR-3129-5p, miR-199b-3p, and miR-4465 in cancer tissues were significantly lower (P<0.001). Compared with high miR-106b-5p, high miR-93-5p, high miR-3129-5p, high miR-199b-3p, high miR-4465 group and low OLR1 group, the low miR-106b-5p, low miR-93-5p, low miR-3129-5p, low miR-199b-3p, low miR-4465 group and high OLR1 group have significantly higher recurrence (all P<0.05) and higher mortality (all P<0.05). The identification value of recurrence assessment model [Y = 4.267+0.336*(miR-106b-5p)+0.168*(miR-93-5p)+1.847*(miR-3129-5p)+2.119*(miR-199b-3p)+0.872*(miR-4465)-3.408*(OLR1)] was high with an AUC of 0.918. The prognosis assessment model [Y = 3.914+0.143*(miR-106b-5p)+0.102*(miR-93-5p)+0.115*(miR-3129-5p)+1.369*(miR-199b-3p)+0.186*(miR-4465)-0.334*(OLR1)] also had high identification value with an AUC of 0.934.

Conclusion. The combined detection of miR-106b-5p, miR-93-5p, miR-3129-5p, miR-199b-3p, miR-4465, and OLR1 is expected to become a molecular biomarker for the long-term prognostic assessment of ovarian cancer.

Key words: Oxidized low-density lipoprotein receptor 1, microRNA, Ovarian cancer, Prognosis

Introduction

Owing to the insidious onset of ovarian cancer and the lack of early diagnosis methods, most patients are in the middle and late stages of the disease when they seek treatment (Aziz et al., 2020). The five-year survival rate for ovarian cancer is less than 45%, making it the seventh most common cancer in women and one of the leading causes of death in gynecologic malignancies (Nahshon et al., 2022). Traditional screening or prognostic methods for ovarian cancer mainly include serum CA-125, color Doppler ultrasound, laparoscopy, cytology, etc. However, due to the low early diagnosis

Corresponding Author: Jun Liu, Department of Gynecology, Hainan General Hospital, No.19, Xiuhua Road, Xiuying District, Haikou, 570311, PR China. e-mail: liujun_haikou@126.com

DOI: 10.14670/HH-18-536

Abbreviations. 3' UTR, 3'untranslated region; DFS, disease-free survival; miRNA, microRNA; OLR1, oxidized low-density lipoprotein receptor 1; qRT-PCR, quantitative real-time polymerase chain reaction.

rate, the combined application is often required.

In recent years, with the deepening of miRNA research, it has been found that miRNAs are involved in the regulation of post-transcriptional expression of more than 30% of human genes (Ghafouri-Fard et al., 2020). MiRNA is a type of highly conserved non-coding single-stranded small RNA with a length of about 19-25nt (Ghafouri-Fard et al., 2020). miRNA degrades the target gene mRNA or inhibits its translation through complete or incomplete pairing with the 3'untranslated region (3' UTR) of the target gene (Ghafouri-Fard et al., 2020). It regulates the expression level of target genes after transcription, thereby participating in the regulation of ontogeny, apoptosis, proliferation, and differentiation (Chen et al., 2020; Ghafouri-Fard et al., 2020; Guo et al., 2020). Recent studies have suggested that miRNAs, as oncogenes or tumor suppressor genes, may play important roles in the gene regulation of the occurrence, development, invasion, metastasis, and angiogenesis of various tumors (Chen et al., 2020; Ghafouri-Fard et al., 2020; Guo et al., 2020), and are related to the occurrence and development of ovarian cancer (An and Yang, 2020; Choi et al., 2020). It is suggested that miRNA may be used as a biomarker or therapeutic target for ovarian cancer and has potential clinical value in the treatment and prognosis of ovarian cancer.

Oxidized low-density lipoprotein receptor 1 (OLR1) plays a key role in the process of endothelial dysfunction induced by oxidized low-density lipoprotein (Jiang et al., 2019). The increased de novo synthesis of fatty acids in tumor cells is a significant feature of the occurrence and development of cancer, and the activation of de novo synthesis is negatively correlated with the prognosis and disease-free survival (DFS) of many types of tumors (Cheng et al., 2019; Jiang et al., 2019; Jin et al., 2021). However, there is no report on the prognostic value of OLR1 and its related miRNAs in ovarian cancer. In this study, first, we detected the protein and mRNA levels of OLR1 in the cancer tissues of patients with ovarian cancer. Next, we applied bioinformatics software and luciferase reporter gene technology to predict and verify the expression profile of miRNAs involved in the regulation of OLR1 and detected the level of miRNAs in cancer tissues. Then, functional experiments were employed to check the biological behaviors of OLR1 and miRNAs in ovarian cancer cells. Furthermore, we analyzed the correlation between the levels of OLR1 and miRNAs in cancer tissues and the clinical characteristics of patients. Finally, we analyzed the relationship between the levels of OLR1 and miRNAs in cancer tissues and the recurrence and 3-year survival of patients with ovarian cancer.

Materials and methods

Enrollment and basic data collection of ovarian cancer patients

From February 2016 to January 2017, 132 patients with ovarian cancer diagnosed in the Department of Gynecology of Hainan General Hospital were included. All patients were diagnosed pathologically. The average age of the patients was (62.11±10.53) years old. All included subjects signed an informed consent form, and the project was approved by the Ethics Committee of Hainan General Hospital (2016013).

Follow-up and analysis of recurrence and survival in ovarian cancer patients

According to the time when the patients were included in the study, they were followed up for 3 years, and the number of deaths during the follow-up period and the corresponding death time were counted. The follow-up endpoint was the death of the patient within 3 years; the patient withdrew from the study within 3 years; the 3-year follow-up ended. In addition, the recurrence rate = the number of recurrences/total number of cases × 100%.

Cell culture and transfection

Ovarian cancer cell lines (A2780, OC3, SKOV-3) and normal ovarian epithelial cell line IOSE80 were cultured in a DMEM medium at a 37°C, 5% CO_2 incubator. MiR-106b-5p, miR-93-5p, miR-3129-5p, miR-199b-3p, and miR-4465 mimics or inhibitors were purchased from Guangzhou Tianyi Huiyuan Gene Technology Co., Ltd.

Cell Counting Kit-8 (CCK-8) assay

After 24h, transfected cells were seeded into a 96-well plate at a density of 1×10^3 per well. Cells were then cultivated for 0, 24, 48, and 72h at 37°C with 5% CO_2. To test cell proliferation, each well of the 96-well plate was loaded with 10 μL CCK-8 solution (Beyotime, Shanghai, China) and incubated at 37°C for 2h. A microplate reader (Tecan Group Ltd., Mannedorf, Switzerland) was used to monitor the absorbance at 450-nm wavelength.

Flow cytometric analysis

The number of ovarian cancer cell apoptosis was detected with an Annexin V-FITC apoptosis detection kit (KeyGen Biotech Co., Ltd., Nanjing, China). Approximately 1×10^6 cells were rinsed with phosphate-buffered saline (PBS) twice, and the supernatant fluid was removed. The collected cells were resuspended in 500 μL binding buffer. Later, 5 μL Annexin V-APC and 5 μL propidium iodide were introduced into the cell suspension, and additional cultivation was performed at room temperature for 15 min without light. Lastly, the late and early apoptotic rates were determined using flow cytometry (Becton Dickinson, San Jose, CA, USA).

Transwell migration and invasion assays

Cell migration was assayed using the Transwell method. Briefly, ovarian cancer cells were detached

using trypsin and rinsed twice with PBS. The upper chambers of 24-well Transwell inserts were covered with about 5×10^4 cells resuspended in 200 μL FBS-free culture medium. A volume of 600 μL culture medium was added to the inferior cavity. Cells were allowed to pass through the porous membrane for 24h. After the removal of cells remaining on the upper surface, the dyeing of migrated cells was done using 0.1% crystal violet for 20 min at room temperature. Images of stained cells were captured using an inverted microscope (Olympus, Tokyo, Japan). Five visuals were chosen at random, and migrated cells that crossed the pores were counted. For the cell invasion assay, the same experimental steps were employed, except that the inserts were pre-coated with Matrigel (BD Biosciences).

Immunohistochemical detection

Paraffin sections were dewaxed, hydrated, and incubated in 3% hydrogen peroxide for 10 min. They were sealed with goat serum for 1h at room temperature, incubated with OLR1 monoclonal antibody at 4°C overnight, incubated with alkaline phosphatase secondary antibody for 1h, and stained with diaminobenzidine and hematoxylin.

Detection of miRNAs and OLR1 mRNA levels in tissues of ovarian cancer patients

Quantitative real-time polymerase chain reaction (qRT-PCR) was performed using RNA reverse transcription and assay kits. U6 and GAPDH are the housekeeping genes of miRNAs and OLR1, respectively. The primer sequence is as follows: OLR1 forward: 5 '-GAACTTGCTCAAGTGCAGGC-3', reverse: 5 '-TTTCGGAATGGCCTCTGTCC-3'; miR-106b-5p: 5′-UAAAGUGCUGACAGUGCAGAU-3′; miR-93-5p forward: 5 '-GCCGCCAAAGTGCTGTTC-3', reverse: 5 '-CAGAGCAGGGTCCGAGGTA-3'; miR-3129-5p: 5 '-GCGCAGTAGTGTAGAGATTG-3'; miR-199b-3p forward: 5 '-CCAGAGGACACCTCCACTCC-3', reverse: 5 '-GGGCTGGGTTAGACCCTCGG-3'; miR-140-3p forward: 5 '-CCTGGTTACCACAGGGTAGA-3', reverse: 5 '-TCAACTGGTGTCGTGGAGTC-3'; miR-4465 forward: 5 '-CUCAAGUAGUCUGAC-3', reverse: 5 '-GTGCAGGGTCCGAGGT-3'; GAPDH forward: 5 '-ACAGTCAGCCGCATCTTCTT-3', reverse: 5 '-AAATGAGCCCCAGCCTTCTC-3'; U6 forward: 5 '-CAGCACATATACTAAAATTGGAACG-3', reverse: 5 '-ACGAATTTGCGTGTCATCC-3'. The relative quantitative method ($2^{-\Delta CT}$ method) was used to calculate the expression level, and each group of samples was repeated three times.

Western blot

Tissue protein was extracted from RIPA lysis buffer and loaded on 10% SDS gel, and then protein was transferred to PVDF membrane. After the membrane was incubated with OLR1 and β-actin primary antibody at 4°C overnight, the PVDF membrane was incubated with secondary antibody for 2h at room temperature to detect the expression level of OLR1.

Statistical analysis

SPSS 19.0 and Graphpad Prism 5.0 were used for analysis. The count data were expressed as a rate (%), and the comparison between groups was performed by chi-square test. The measurement data were expressed as mean ± standard deviation (SD). The receiver operator characteristic curve (ROC) was used to compare the area under the ROC curve (AUC) and 95% confidence interval (CI). Kaplan Meier method was used to analyze the survival curve. The multivariate analysis including the variables with a $P<0.05$ in univariate analysis was used to assess the Cox proportional hazards model.

Results

OLR1 expression in ovarian cancer tissue is significantly increased and is related to the malignant biological behavior of the tumor and poor prognosis

Compared with adjacent tissues, OLR1 protein in ovarian cancer tissues was significantly higher ($P<0.001$, Fig. 1A,B). Compared with adjacent tissues, OLR1 mRNA levels in ovarian cancer tissues were significantly higher ($P<0.05$, Fig. 1C). Compared with the low OLR1 group, the high OLR1 group had significantly higher mortality ($P<0.05$, Fig. 1D). The relatively higher OLR1 expression was detected in the SKOV-3 cell line, which was thus selected as the subject of subsequent experiments (Fig. 1E).

To ascertain whether OLR1 is involved in the tumorigenesis of ovarian cancer, si-OLR1 or si-NC was transfected into SKOV-3 cells to knockdown endogenous OLR1 expression. OLR1 knockdown was verified by qRT-PCR (Fig. 2A). si-OLR1#1 presented higher silencing efficiency, thus, the siRNA was used in the following experiments. The effects of OLR1 on ovarian cancer cell proliferation and apoptosis were assessed by CCK-8 assay and flow cytometric analysis, respectively. Transfection with si-OLR1 caused an obvious decrease in proliferation rate (Fig. 2B) and an increase in apoptosis rate (Fig. 2C) in SKOV-3 cells. Furthermore, the migratory (Fig. 2D) and invasive (Fig. 2E) properties of SKOV-3 cells were strikingly hindered by si-OLR1 treatment in contrast to the si-NC treatment. Overall, the observations mentioned above supported the conclusion that OLR1 acts as an oncogene in ovarian cancer.

MiR-106b-5p, miR-93-5p, miR-3129-5p, miR-199b-3p, and miR-4465 are involved in the regulation of OLR1 expression

We then used PicTar (https://pictar.mdc-berlin.de/), miRanda (http://www.microrna.org/), miRDB (http://

ww.mirdb.org/), and Targetscan (Http://www.targetscan.org/) online prediction systems, and found out the miRNA profiles predicted by each system with OLR1 as the target protein, and used a Venn diagram to analyze the miRNA profiles jointly predicted by the four software models (Fig. 2F). A total of 6 miRNAs were predicted, namely miR-106b-5p, miR-93-5p, miR-3129-5p, miR-140-3p, miR-199b-3p, and miR-4465.

Finally, we performed the dual-luciferase reporter analysis to verify the targeting relationship between the six miRNAs and OLR1, as shown in Figs. 3, 4. We found that in addition to miR-140-3p (Fig. 3A), after transferring miR-199b-3p (Fig. 3B), miR-4465 (Fig. 3C), miR-106b-5p (Fig. 4A), miR-93-5p (Fig. 4B), or miR-3129-5p (Fig. 4C) to SKOV-3, the luciferase activity was significantly reduced ($P<0.05$), and the expression level of OLR1 protein in SKOV-3 cells was also significantly reduced ($P<0.05$, Figs. 3, 4). Then, we chose miR-106b-5p, miR-93-5p, miR-3129-5p, miR-199b-3p and miR-4465 for further research.

miR-106b-5p, miR-93-5p, miR-3129-5p, miR-199b-3p, and miR-4465 expressions in ovarian cancer tissue are significantly decreased, and are related to good prognosis

Firstly, transfection with miR-106b-5p, miR-93-5p, miR-3129-5p, miR-199b-3p, and miR-4465 mimics caused an obvious decrease in proliferation rate (Fig. 5A) and an increase in apoptosis rate (Fig. 5B) in SKOV-3 cells. Furthermore, the migratory (Fig. 5C) and invasive (Fig. 5D) properties of SKOV-3 cells were strikingly hindered in contrast to the NC mimic

Table 1. The relationship between miR-106b-5p, miR-93-5p, miR-3129-5p, miR-199b-3p, miR-4465, OLR1 levels in cancer tissues and 36-month recurrence and mortality rate in ovarian cancer patients.

Indicators	Recurrence rate (%)			OS (%)		
	No. (%)	χ^2	P	No. (%)	χ^2	P
miR-106b-5p		9.943	0.002		3.918	0.048*
>median	7 (10.6%)			3 (4.5%)		
≤median	22 (33.3%)			11 (16.7%)		
miR-93-5p		11.313	0.001		6.472	0.011*
>median	5 (7.6%)			2 (3.0%)		
≤median	24 (36.4%)			12 (18.2%)		
miR-3129-5p		5.347	0.021		3.918	0.048*
>median	9 (13.6%)			3 (4.5%)		
≤median	20 (30.3%)			11 (16.7%)		
miR-199b-3p		12.771	<0.001		6.472	0.011*
>median	6 (9.1%)			2 (3.0%)		
≤median	23 (34.8%)			12 (18.2%)		
miR-4465		7.468	0.006		3.918	0.048*
>median	8 (12.1%)			3 (4.5%)		
≤median	21 (31.8%)			11 (16.7%)		
OLR1		15.953	<0.001		6.472	0.011*
>median	24 (36.4%)			12 (18.2%)		
≤median	5 (7.6%)			2 (3.0%)		

OS, overall survival rate; OLR1, oxidized low-density lipoprotein receptor 1. *P-value was calculated by Fisher's exact test.

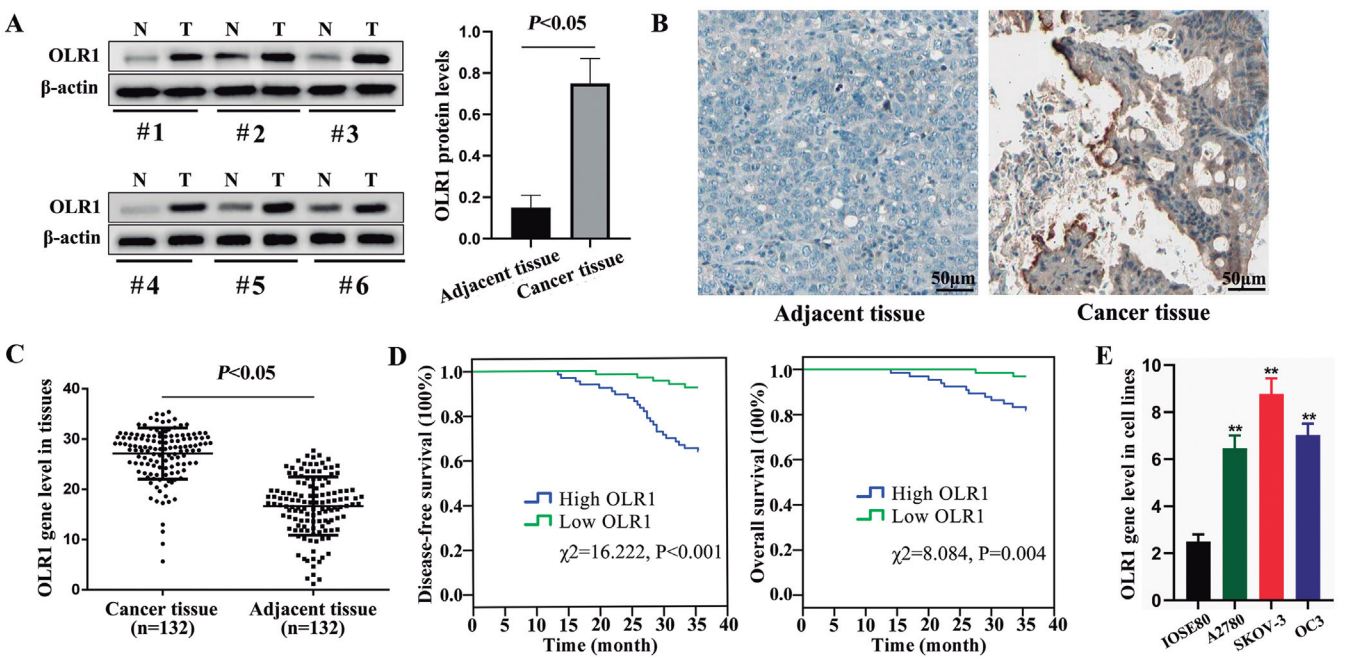

Fig. 1. OLR1 protein and mRNA levels in ovarian cancer and adjacent tissues. **A-C.** Compared with adjacent tissues, the level of OLR1 protein in cancer tissues was significantly higher (**A.** Western blot analysis; **B.** Immunohistochemical staining analysis; **C.** qRT-PCR analysis). **D.** Compared with the low OLR1 group, the high OLR1 group has significant mortality ($P<0.05$). **E.** The relatively higher OLR1 expression was detected in the SKOV-3 cell line. *$P<0.05$, compared to the control.

treatment.

Next, we detected miR-106b-5p, miR-93-5p, miR-3129-5p, miR-140-3p, miR-199b-3p, and miR-4465 expression levels in 132 pairs of ovarian cancer and adjacent tissues, respectively, and analyzed their correlation with OLR1 gene levels in cancer tissues (Fig. 6). Compared with adjacent tissues, the levels of miR-106b-5p (Fig. 6A), miR-93-5p (Fig. 6B), miR-3129-5p (Fig. 6C), miR-199b-3p (Fig. 6E), and miR-4465 (Fig. 6F) in cancer tissues were significantly lower (P<0.05), while there was no significant difference in the expression of miR-140-3p in cancer and adjacent tissues (*P*=0.169, Fig. 6D). Interestingly, the levels of miR-106b-5p (*r*=-0.521, *P*<0.001, Fig. 6G), miR-93-5p (*r*=-0.509, *P*<0.001, Fig. 6H), miR-3129-5p (*r*=-0.464, *P*<0.001, Fig. 6I), miR-199b-3p (*r*=-0.482, *P*<0.001, Fig. 6K), and miR-4465 (*r*=-0.449, *P*<0.001, Fig. 6L) were all significantly negatively correlated with OLR1 (*P*<0.001). There was no significant correlation between miR-140-3p level and OLR1 (*r*=-0.021, *P*=0.864, Fig. 6J).

Furthermore, the relationship between miR-106b-5p, miR-93-5p, miR-3129-5p, miR-199b-3p, miR-4465, OLR1 levels and 36-month recurrence and mortality rate

Table 2. Prognostic factors in Cox proportional hazards model.

Factors	Univariate analysis		Multivariate analysis	
	HR (95% CI)	P	HR (95% CI)	P
Age	2.370 (0.402-4.189)	0.468		
Alcoholism	0.910 (0.443-1.816)	0.791		
miR-106b-5p	0.763 (0.552-0.942)	0.011	0.694 (0.586-0.821)	0.004
miR-93-5p	0.796 (0.509-0.984)	0.031	0.875 (0.753-0.994)	0.042
miR-3129-5p	0.703 (0.465-0.925)	0.008	0.726 (0.524-0.936)	0.013
miR-199b-3p	0.815 (0.754-0.963)	0.024	0.665 (0.462-0.870)	<0.001
miR-4465	0.774 (0.601-0.950)	0.016	0.672 (0.546-0.815)	0.003
OLR1	3.022 (1.358-6.656)	0.003	3.145 (1.398-7.165)	<0.001

OLR1, oxidized low-density lipoprotein receptor 1; HR, Hazard ratio; CI, confidence interval.

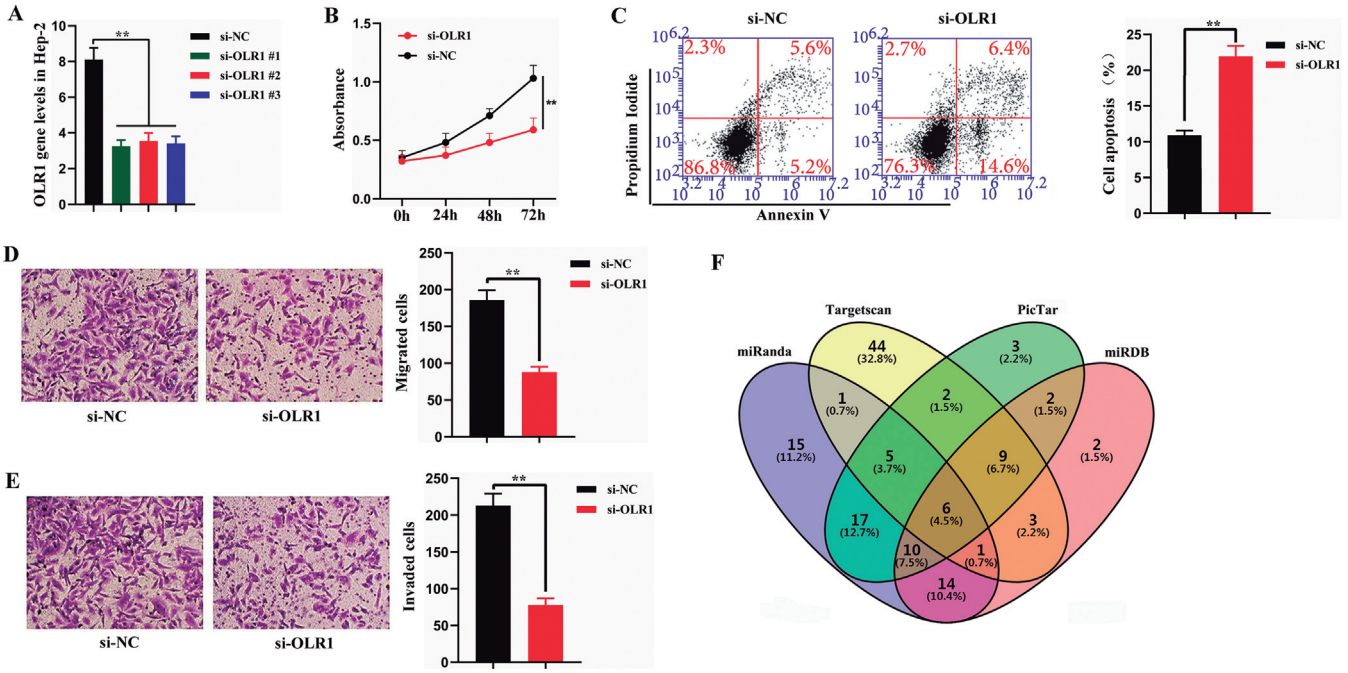

Fig. 2. OLR1 expression in ovarian cancer is related to the malignant biological behavior of the tumor. **A.** SKOV-3 cell line was transfected with si-OLR1#1 or si-OLR1#2, or si-OLR1#3 and then subjected to qRT-PCR for silencing efficiency determination. **B.** CCK-8 assay detected the change of proliferative capacity in the SKOV-3 cell line after the introduction of si-OLR1. **C.** Apoptosis of SKOV-3 cells transfected with si-OLR1 was evaluated by flow cytometric analysis. **D, E.** Transwell migration and invasion assays were performed to assess the effect of OLR1 interference on the migration and invasion of SKOV-3 cells. **F.** Venn diagram was used to explore the miRNAs by PicTar, miRanda, miRDB, and Targetscan. ***P*<0.01, compared to the control.

in ovarian cancer patients are listed in Table 1. According to the median of miR-106b-5p, miR-93-5p, miR-3129-5p, miR-199b-3p, miR-4465 and OLR1 in cancer tissues, patients were divided into high/low expression groups. Compared with high miR-106b-5p, high miR-93-5p, high miR-3129-5p, high miR-199b-3p, high miR-4465 group and low OLR1 group, the low miR-106b-5p, low miR-93-5p, low miR-3129-5p, low miR-199b-3p, low miR-4465 group and high OLR1 group have significantly higher recurrence (all $P<0.05$) and higher mortality (all $P<0.05$).

Survival analysis of miR-106b-5p, miR-93-5p, miR-3129-5p, miR-199b-3p, miR-4465, and OLR1 on the recurrence and prognosis of ovarian cancer patients

All patients were followed up for three years. There were 29 relapses and 14 deaths. We analyzed the correlation between miR-106b-5p, miR-93-5p, miR-3129-5p, miR-199b-3p, miR-4465, and OLR1 and the prognosis of patients. Survival analysis results are shown in Fig. 7. Compared with high miR-106b-5p, high miR-93-5p, high miR-3129-5p, high miR-199b-3p, and high miR-4465 group, the DFS and overall survival (OS) of patients with low miR-106b-5p (Fig. 7A,F), low miR-93-5p (Fig. 7B,G), low miR-3129-5p (Fig. 7C,H), low miR-199b-3p (Fig. 7D,I), and low miR-4465 group (Fig. 7E,J) were significantly reduced (all $P<0.05$). Then, we confirmed that miR-106b-5p, miR-93-5p, miR-3129-5p, miR-199b-3p, miR-4465, and OLR1 were independent prognostic predictors for overall survival of ovarian cancer patients by multivariate analysis using Cox regression model ($P<0.05$, Table 2).

The predictive value of miR-106b-5p, miR-93-5p, miR-3129-5p, miR-199b-3p, miR-4465, and OLR1 in the occurrence of recurrence and prognosis in ovarian cancer patients

The detailed information of recurrence and

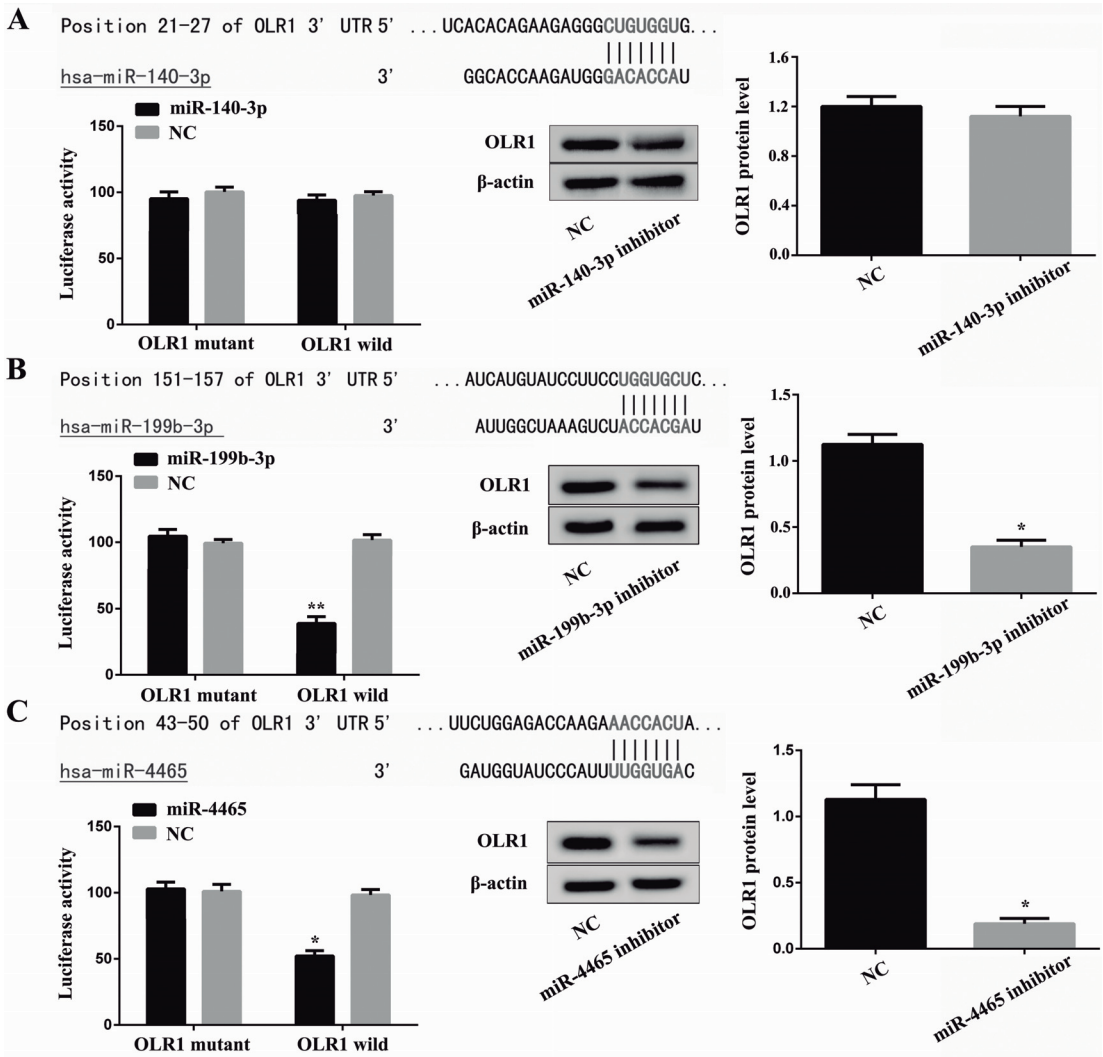

Fig. 3. MiR-199b-3p and miR-4465 are involved in the regulation of OLR1 expression. **A.** Luciferase reporter gene method and Western blot analysis were used to verify the relationship between miR-140-3p and OLR1. **B.** Luciferase reporter gene method and Western blot analysis were used to verify the relationship between miR-199b-3p and OLR1. **C.** Luciferase reporter gene method and Western blot analysis were used to verify the relationship between miR-4465 and OLR1. **P*<0.05, compared to the control; ***P*<0.01, compared to the control.

prognosis performances is listed in Table 3. The recurrence assessment model was: Y = 4.267+ 0.336*(miR-106b-5p)+0.168*(miR-93-5p)+1.847*(miR-3129-5p)+2.119*(miR-199b-3p)+0.872*(miR-4465)-3.408*(OLR1). The identification value of this model was high with an AUC of 0.918 (Fig. 8A, Table 3). Moreover, the prognosis assessment model was: Y = 3.914+0.143*(miR-106b-5p)+0.102*(miR-93-5p)+0.115*(miR-3129-5p)+1.369*(miR-199b-3p)+ 0.186*(miR-4465)-0.334*(OLR1). The identification value of this model was high with an AUC of 0.934 (Fig. 8B, Table 3).

Discussion

At present, the treatment of ovarian cancer has been greatly improved, including surgical resection, adjuvant therapy, and interventional therapy. However, because many ovarian cancer patients are diagnosed after the appearance of relevant clinical symptoms, this results in a low 5-year survival rate for patients. Some scholars have pointed out that if effective molecular markers can be found for early monitoring, the 5-year survival rate of ovarian cancer patients will increase (Cai et al., 2021; Chen et al., 2021).

A large number of studies have found that, in addition to promoting the formation of atherosclerotic plaque, OLR1 also has a significant tumor-promoting effect, and has revealed its potential cancer-promoting mechanism (Jiang et al., 2019). The Cancer Gene Atlas data indicates that the life expectancy of prostate cancer patients is significantly correlated with the level of OLR1, and the median survival of patients with high OLR1 expression decreased by nearly 2 years among patients with low OLR1 expression (Wan et al., 2015). The above studies suggest that the up-regulation of OLR1 expression in tissues is an important factor in promoting tumor formation.

MiRNA plays a regulatory function by silencing downstream molecules. In the current study, four online

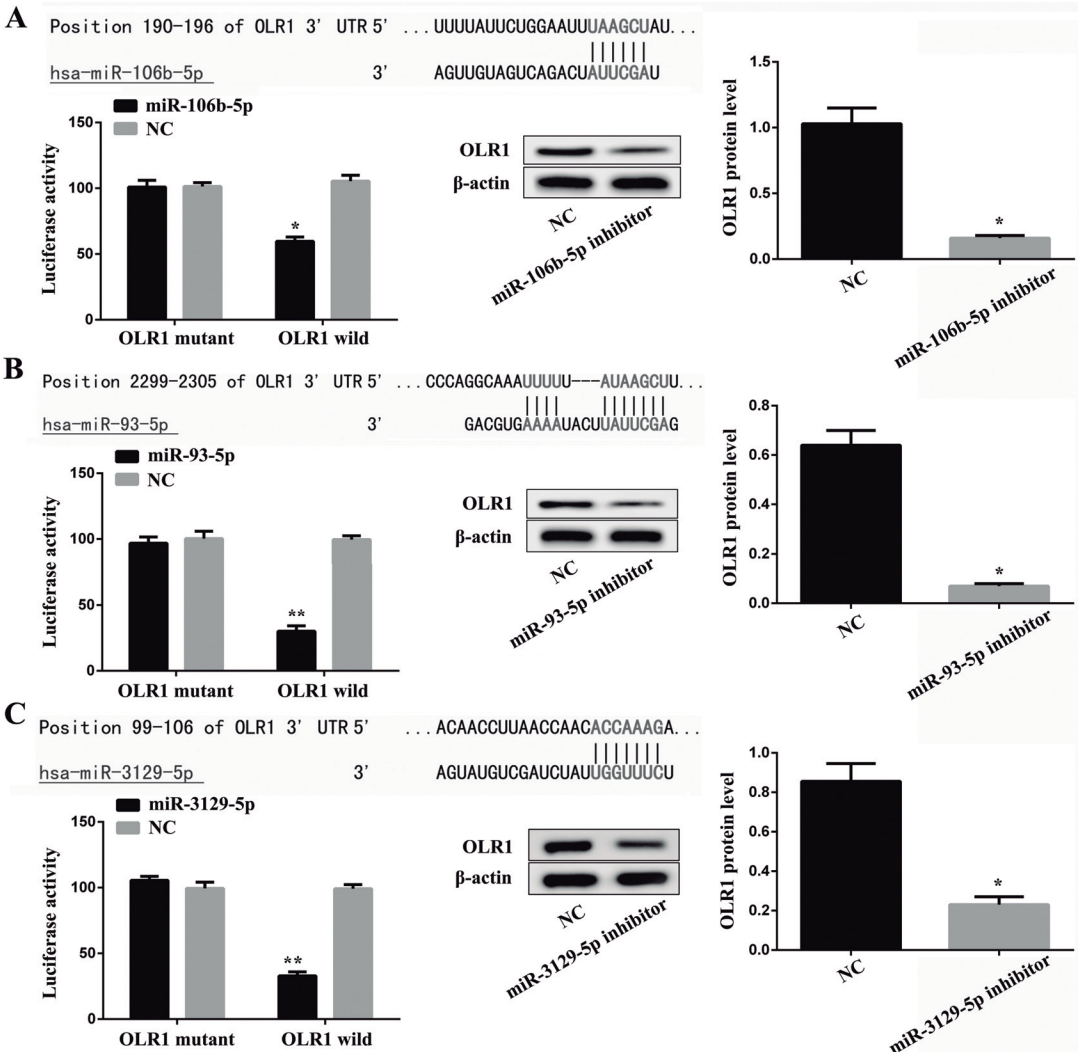

Fig. 4. MiR-106b-5p, miR-93-5p, and miR-3129-5p are involved in the regulation of OLR1 expression. **A.** Luciferase reporter gene method and Western blot analysis were used to verify the relationship between miR-106b-5p and OLR1. **B.** Luciferase reporter gene method and Western blot analysis were used to verify the relationship between miR-93-5p and OLR1. **C.** Luciferase reporter gene method and Western blot analysis were used to verify the relationship between miR-3129-5p and OLR1. **P*<0.05, compared to the control; ***P*<0.01, compared to the control.

prediction software models were used to screen out 5 miRNAs that target and regulate OLR1, including miR-106b-5p, miR-93-5p, miR-3129-5p, miR-199b-3p, and miR-4465. The detection of the luciferase reporter gene verified that the above 5 miRNAs are involved in the targeted regulation of OLR1, and the 5 miRNAs have also been found to function as tumor suppressor genes in the clinical and basic research of a variety of tumors (Ni et al., 2018). Ni et al. (2018) found that miR-106b-5p inhibited the invasion and metastasis of colorectal cancer cells by inhibiting the expression of cathepsin A. Ling et al. (2021) reported that miR-106b-5p inhibited the growth and progression of lung adenocarcinoma cells by downregulating IGSF10. Xiang et al. (2017) found that miR-93-5p inhibited the epithelial-mesenchymal transition of breast cancer cells by targeting myocardin-like 1 and signal transducer and activator of transcription 3 *in vitro*. Long et al. (2019) found that LncRNA MALAT1 mediated the progression of hepatocellular carcinoma via lowering miR-3129-5p expression. Koshizuka et al. (2017) analyzed the miRNA expression signature by RNA sequencing, and their results showed that the miR-199 family (miR-199a-5p, miR-199a-3p, miR-199b-5p, and miR-199b-3p) was significantly reduced in cancer tissues. Sun et al. (2017) found that miR-4465 suppressed cancer cell proliferation and metastasis by directly targeting the oncogene EZH2 in non-small cell lung cancer. In this study, 132 pairs of ovarian cancer patients were included. It was found that

Table 3. The predictive value of miR-106b-5p, miR-93-5p, miR-3129-5p, miR-199b-3p, miR-4465, and OLR1 in the prognosis for ovarian cancer patients.

Model	AUC (95% CI)	Sensitivity/Specificity	P
Recurrence assessment model			
miR-106b-5p	0.648 (0.599-0.697)	40.2/100	<0.001
miR-93-5p	0.893 (0.864-0.922)	78.4/88.3	<0.001
miR-3129-5p	0.864 (0.829-0.899)	91.1/73.6	<0.001
miR-199b-3p	0.697 (0.649-0.744)	76.1/58.9	<0.001
miR-4465	0.702 (0.593-0.814)	54.5/83.2	<0.001
OLR1	0.796 (0.755-0.837)	68.3/90.9	<0.001
Recurrence model	0.918 (0.891-0.944)	84.6/90.4	<0.001
Prognosis assessment model			
miR-106b-5p	0.843 (0.805-0.880)	78.9/84.2	<0.001
miR-93-5p	0.684 (0.635-0.732)	50.6/92.7	<0.001
miR-3129-5p	0.797 (0.754-0.840)	72.1/86.6	<0.001
miR-199b-3p	0.881 (0.849-0.912)	87.2/59.3	<0.001
miR-4465	0.792 (0.751-0.832)	57.8/84.6	<0.001
OLR1	0.747 (0.702-0.792)	67.6/83.7	<0.001
Prognosis model	0.934 (0.909-0.958)	86.9/99.8	<0.001

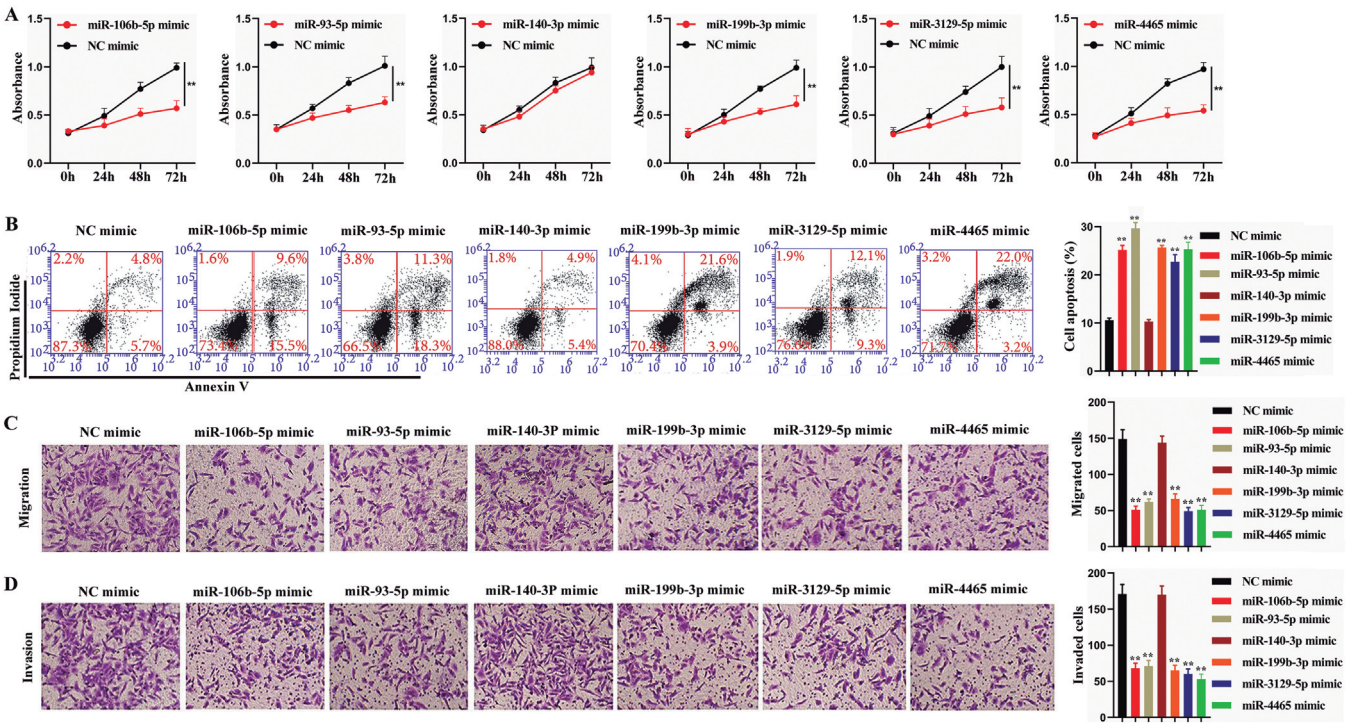

Fig. 5. Effects of miR-106b-5p, miR-93-5p, miR-3129-5p, miR-199b-3p, and miR-4465 on SKOV-3 cell malignant biological behavior. **A.** CCK-8 assay detected the change of proliferative capacity in SKOV-3 cell line after the introduction of miR-106b-5p or miR-93-5p or miR-3129-5p or miR-199b-3p or and miR-4465 mimic. **B.** Apoptosis rate of SKOV-3 cell transfected with miR-106b-5p or miR-93-5p or miR-3129-5p or miR-199b-3p or and miR-4465 mimic was evaluated by flow cytometric analysis. **C, D.** Transwell migration and invasion assays were performed to assess the effect of miR-106b-5p or miR-93-5p or miR-3129-5p or miR-199b-3p or and miR-4465 mimic interference on the migration and invasion of SKOV-3 cells. ***P*<0.01, compared to the control.

the levels of miR-106b-5p, miR-93-5p, miR-3129-5p, miR-199b-3p, and miR-4465 in the cancer tissues of ovarian cancer patients were significantly lower than those in the adjacent tissues. It is consistent with the results of previous studies (Koshizuka et al., 2017; Sun et al., 2017; Xiang et al., 2017; Ni et al., 2018; Ghafouri-Fard et al., 2020). Further analysis revealed that low miR-106b-5p, low miR-93-5p, low miR-3129-5p, low miR-199b-3p, low miR-4465, and high OLR1 levels were positively correlated with recurrence rate and

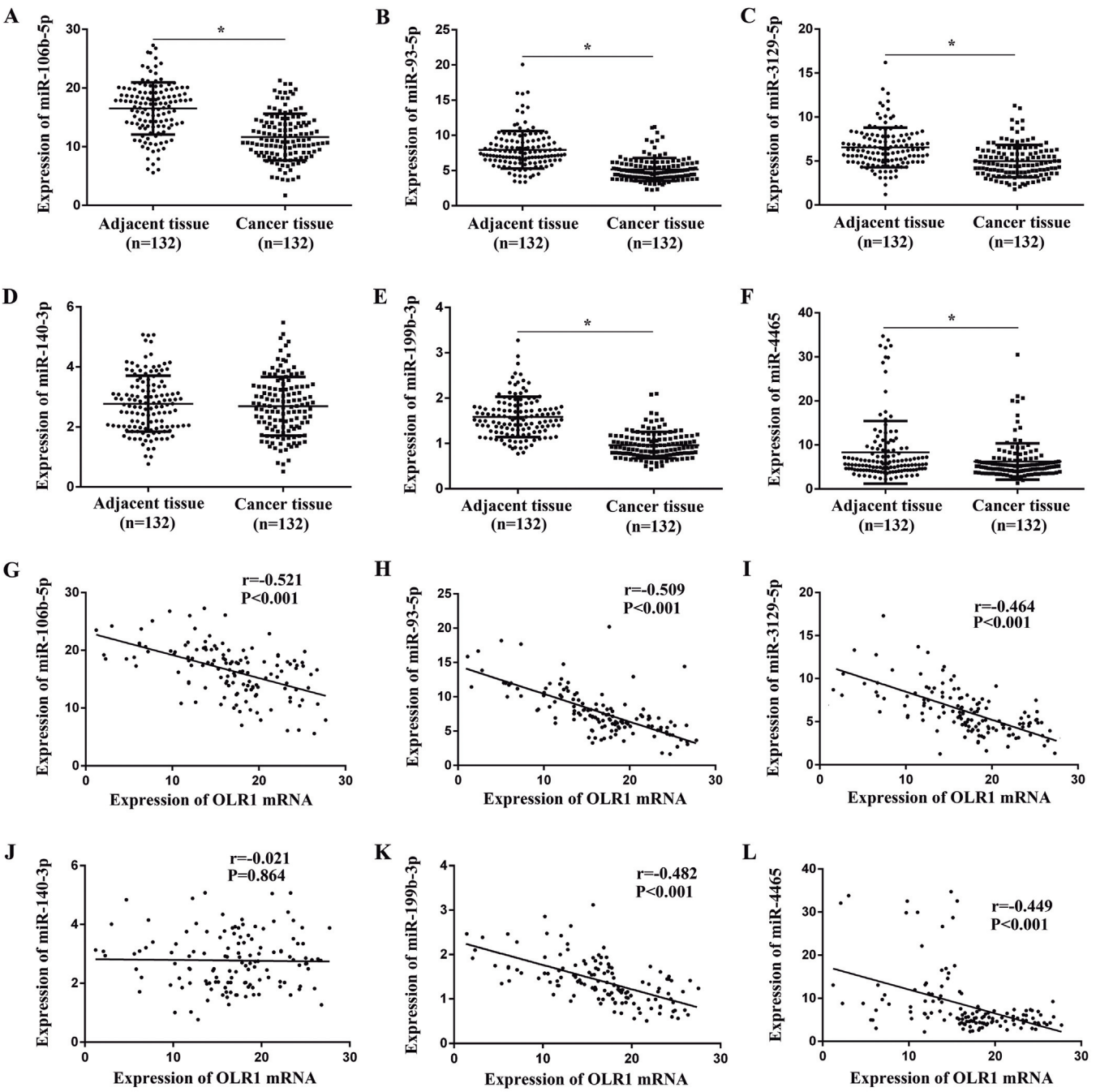

Fig. 6. Expression of miR-106b-5p, miR-93-5p, miR-3129-5p, miR-199b-3p, and miR-4465 in ovarian cancer and its correlation with OLR1 mRNA. Compared with adjacent tissues, the levels of miR-106b-5p **(A)**, miR-93-5p **(B)**, miR-3129-5p **(C)**, miR-199b-3p **(E)**, and miR-4465 **(F)** in cancer tissues were significantly lower (P<0.001), while there was no significant difference in the expression of miR-140-3p in cancer and adjacent tissues **(D)**. The levels of miR-106b-5p **(G)**, miR-93-5p **(H)**, miR-3129-5p **(I)**, miR-199b-3p **(K)**, and miR-4465 **(L)** were all significantly negatively correlated with OLR1 (P<0.001). There was no significant correlation between miR-140-3p level and OLR1 **(J)**. *P<0.05, compared to adjacent tissues.

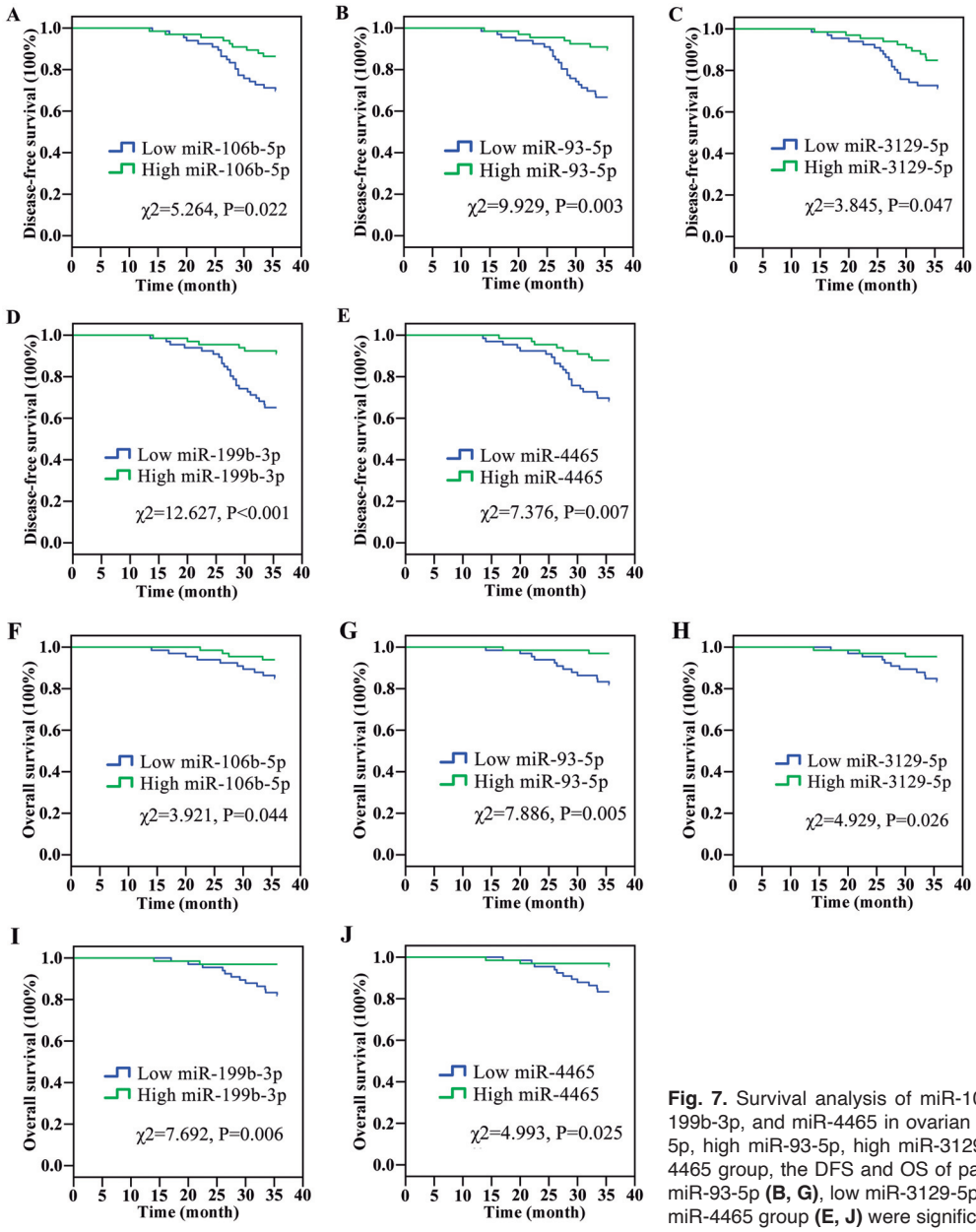

Fig. 7. Survival analysis of miR-106b-5p, miR-93-5p, miR-3129-5p, miR-199b-3p, and miR-4465 in ovarian cancer. Compared with high miR-106b-5p, high miR-93-5p, high miR-3129-5p, high miR-199b-3p, and high miR-4465 group, the DFS and OS of patients with low miR-106b-5p **(A, F)**, low miR-93-5p **(B, G)**, low miR-3129-5p **(C, H)**, low miR-199b-3p **(D, I)**, and low miR-4465 group **(E, J)** were significantly reduced (all $P<0.05$).

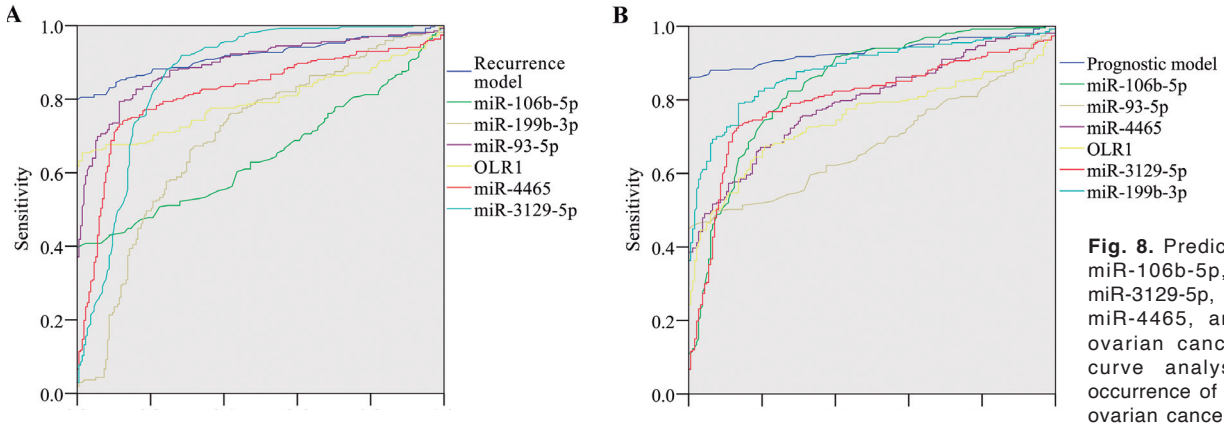

Fig. 8. Predictive value of miR-106b-5p, miR-93-5p, miR-3129-5p, miR-199b-3p, miR-4465, and OLR1 in ovarian cancer. **A.** ROC curve analysis for the occurrence of recurrence in ovarian cancer patients. **B.** ROC curve analysis for the prognostic evaluation in ovarian cancer patients.

mortality. Furthermore, we used ROC analysis to analyze multiple combinations of the above 6 marker molecules. The results showed that the specificity for predicting recurrence was 90.4%, and the sensitivity was 84.6%; the specificity for predicting prognosis was 99.8%, and the sensitivity was 86.9%. The above studies suggest that different combinations of miR-106b-5p, miR-93-5p, miR-3129-5p, miR-199b-3p, miR-4465, and OLR1 in cancer tissues have value in the evaluation of ovarian cancer recurrence and prognosis.

In summary, our research provides novel ideas for the treatment and prognosis improvement of ovarian cancer patients. The combined detection of miR-106b-5p, miR-93-5p, miR-3129-5p, miR-199b-3p, miR-4465, and OLR1 is expected to become a molecular biomarker for the long-term prognostic assessment of ovarian cancer.

Acknowledgements. None.
Conflict of interest statement. None declared.

References

An Y. and Yang Q. (2020). MiR-21 modulates the polarization of macrophages and increases the effects of M2 macrophages on promoting the chemoresistance of ovarian cancer. Life Sci. 242, 117162.

Aziz N.B., Mahmudunnabi R.G., Umer M., Sharma S., Rashid M.A., Alhamhoom Y., Shim Y.B., Salomon C. and Shiddiky M.J.A. (2020). MicroRNAs in ovarian cancer and recent advances in the development of microRNA-based biosensors. Analyst 145, 2038-2057.

Cai L., Ye L., Hu X., He W., Zhuang D., Guo Q., Shu K. and Jie Y. (2021). MicroRNA miR-330-3p suppresses the progression of ovarian cancer by targeting RIPK4. Bioengineered 12, 440-449.

Chen W., Du J., Li X., Zhi Z. and Jiang S. (2020). microRNA-137 downregulates MCL1 in ovarian cancer cells and mediates cisplatin-induced apoptosis. Pharmacogenomics 21, 195-207.

Chen Z., Xiao Z., Zeng S. and Yan Z. (2021). The potential value of microRNA-145 for predicting prognosis in patients with ovarian cancer: A protocol for systematic review and meta-analysis. Medicine (Baltimore) 100, e26922.

Cheng S., Wang G., Wang Y., Cai L., Qian K., Ju L., Liu X., Xiao Y. and Wang X. (2019). Fatty acid oxidation inhibitor etomoxir suppresses tumor progression and induces cell cycle arrest via PPARγ-mediated pathway in bladder cancer. Clin. Sci (Lond). 133, 1745-1758.

Choi P.W., So W.W., Yang J., Liu S., Tong K.K., Kwan K.M., Kwok J.S., Tsui S.K.W., Ng S.K., Hales K.H., Hales D.B., Welch W.R., Crum C.P., Fong W.P., Berkowitz R.S. and Ng S.W. (2020). MicroRNA-200 family governs ovarian inclusion cyst formation and mode of ovarian cancer spread. Oncogene 39, 4045-4060.

Ghafouri-Fard S., Shoorei H. and Taheri M. (2020). miRNA profile in ovarian cancer. Exp. Mol. Pathol. 113, 104381.

Guo J.Y., Wang X.Q. and Sun L.F. (2020). MicroRNA-488 inhibits ovarian cancer cell metastasis through regulating CCNG1 and p53 expression. Eur. Rev. Med. Pharmacol. Sci. 24, 2902-2910.

Jiang L., Jiang S., Zhou W., Huang J., Lin Y., Long H. and Luo Q. (2019). Oxidized low density lipoprotein receptor 1 promotes lung metastases of osteosarcomas through regulating the epithelial-mesenchymal transition. J. Transl. Med. 17, 369.

Jin Z., Chai Y.D. and Hu S. (2021). Fatty acid metabolism and cancer. Adv. Exp. Med. Biol. 1280, 231-241.

Koshizuka K., Hanazawa T., Kikkawa N., Arai T., Okato A., Kurozumi A., Kato M., Katada K., Okamoto Y. and Seki N. (2017). Regulation of ITGA3 by the anti-tumor miR-199 family inhibits cancer cell migration and invasion in head and neck cancer. Cancer Sci. 108, 1681-1692.

Lee A.W. (2018). Oxidized low-density lipoprotein-deteriorated psoriasis is associated with the upregulation of Lox-1 receptor and Il-23 expression *in vivo* and *in vitro*. Int. J. Mol. Sci. 19, 2610.

Ling B., Liao X., Tang Q., Ye G., Bin X., Wang J., Pang Y. and Qi G. (2021). MicroRNA-106b-5p inhibits growth and progression of lung adenocarcinoma cells by downregulating IGSF10. Aging (Albany NY) 13, 18740-18756.

Long L., Xiang H., Liu J., Zhang Z. and Sun L. (2019). ZEB1 mediates doxorubicin (Dox) resistance and mesenchymal characteristics of hepatocarcinoma cells. Exp. Mol. Pathol. 106, 116-122.

Nahshon C., Barnett-Griness O., Segev Y., Schmidt M., Ostrovsky L. and Lavie O. (2022). Five-year survival decreases over time in patients with BRCA-mutated ovarian cancer: a systemic review and meta-analysis. Int. J. Gynecol. Cancer 32, 48-54.

Ni S., Weng W., Xu M., Wang Q., Tan C., Sun H., Wang L., Huang D., Du X. and Sheng W. (2018). miR-106b-5p inhibits the invasion and metastasis of colorectal cancer by targeting CTSA. Onco. Targets Ther. 11, 3835-3845.

Shih C.M., Huang C.Y., Wang K.H., Huang C.Y., Wei P.L., Chang Y.J., Hsieh C.K., Liu K.T. and Sun X., Fu X., Xu S., Qiu P., Lv Z., Cui M., Zhang Q. and Xu Y. (2021). OLR1 is a prognostic factor and correlated with immune infiltration in breast cancer. Int. Immunopharmacol. 101(Pt B), 108275.

Sun J., Tian X., Lu S.Q. and Hu H.B. (2017). MicroRNA-4465 suppresses tumor proliferation and metastasis in non-small cell lung cancer by directly targeting the oncogene EZH2. Biomed. Pharmacother. 96, 1358-1362.

Wan F., Qin X., Zhang G., Lu X., Zhu Y., Zhang H., Dai B., Shi G. and Ye D. (2015). Oxidized low-density lipoprotein is associated with advanced-stage prostate cancer. Tumour Biol. 36, 3573-3582.

Xiang Y., Liao X.H., Yu C.X., Yao A., Qin H., Li J.P., Hu P., Li H., Guo W., Gu C.J. and Zhang T.C. (2017). MiR-93-5p inhibits the EMT of breast cancer cells via targeting MKL-1 and STAT3. Exp. Cell Res. 357, 135-144.

Accepted October 20, 2022